EXHIBIT 0

Stocker et al., *Nat Cell Biol* 5: 559-565 (2003)

nature
cell biology

Rheb is an essential regulator of S6K in controlling cell growth in *Drosophila*

Hugo Stocker[1], Thomas Radimerski[2], Benno Schindelholz[3], Franz Wittwer[1], Priyanka Belawat[1], Pierre Daram[3], Sebastian Breuer[3], George Thomas[2] and Ernst Hafen[1]

Understanding the mechanisms through which multicellular organisms regulate cell, organ and body growth is of relevance to developmental biology and to research on growth-related diseases such as cancer. Here we describe a new effector in growth control, the small GTPase Rheb (Ras homologue enriched in brain). Mutations in the *Drosophila melanogaster Rheb* gene were isolated as growth-inhibitors, whereas overexpression of *Rheb* promoted cell growth. Our genetic and biochemical analyses suggest that Rheb functions downstream of the tumour suppressors Tsc1 (tuberous sclerosis 1)–Tsc2 in the TOR (target of rapamycin) signalling pathway to control growth, and that a major effector of Rheb function is ribosomal S6 kinase (S6K).

A growing number of studies in genetically tractable model organisms, such as *D. melanogaster*, have greatly enhanced our understanding of growth regulation. From these efforts, two highly conserved signalling pathways dedicated to the control of growth have emerged, namely the insulin receptor (InR)/phosphatidylinositol-3-OH kinase (PI(3)K) and TOR pathways[1,2]. Recent studies have also shown that these two pathways interact, although the mechanisms by which they communicate are the subject of controversy[3,4]. In addition, each pathway seems to be modulated by distinct tumour suppressor genes, *PTEN* (phosphatase and tensin homologue deleted in chromosome 10) and *TSC1–TSC2*, respectively[5,6]. Whereas it is clear that PTEN constrains PI(3)K signalling by dephosphorylation of phosphatidylinositol-3,4,5-triphosphate ($PtdInsP_3$)[7], the mechanism by which TSC1 and TSC2 counteract TOR signalling remains elusive. Importantly, TSC2 possesses a putative GTPase-activating protein (GAP) domain, which has been shown to increase the intrinsic GTPase activity of the small GTPases Rap1 and Rab5 (refs 8, 9). Here, we present genetic and biochemical data from *Drosophila* suggesting a novel role for the small GTPase Rheb in the TOR/S6K signalling pathway.

To identify growth-regulating genes, we performed two complementary screens for loss- and gain-of-function mutations, respectively. In the loss-of-function screen, we discovered a novel complementation group of ten alleles that impair cell and organ growth. The ethylmethane sulphonate (EMS)-induced mutations were identified on the basis of reduced head size of mosaic animals, consisting of heads largely made up of homozygous mutant cells and bodies containing heterozygous cells (compare Fig. 1a with Fig. 1b)[10,11]. This phenotype is reminiscent of mutations in InR signalling components. Genetic mapping of two representative alleles and subsequent testing of candidate open reading frames identified alterations in the gene *CG1081* in seven alleles. *CG1081* encodes a small GTPase most closely related to mammalian Rheb[12] (Supplementary Information, Fig. S1a). Therefore, we named this complementation group *Rheb*.

The gain-of-function screen for genes that stimulate growth when overexpressed resulted in the identification of an EP element in the *Rheb* locus (EP 50.084). EP-mediated overexpression of *Rheb* in the developing eye substantially increased eye size (Fig. 1c). We generated six additional *Rheb* loss-of-function alleles by imprecise excision of EP 50.084. Whereas all combinations of the EMS-induced *Rheb* alleles were lethal, some hetero-allelic combinations of EMS-induced alleles and EP excision alleles were viable and resulted in flies of reduced size (Supplementary Information, Fig. S1b). The size reduction was caused by a decrease in cell number (3–11%), as well as in cell size (9–14% in wing cells, more than 20% in eye cells as judged by ommatidial size). In addition, the small flies eclosed with a delay of at least one day and the females had rudimentary ovaries and were sterile (Fig. 1d). Thus, the surviving *Rheb* mutant flies display all the hallmarks of impaired InR signalling activity, resembling flies lacking the insulin-receptor substrate (IRS) protein Chico[10].

A more severe reduction in Rheb function (in heteroallelic combinations of *Rheb* mutations) was lethal at late larval or early pupal stages. Mutant larvae and pupae were consistently smaller (Fig. 1e, f), although the phenotype was variable. Interestingly, the size reduction was more pronounced in the endoreplicative larval tissue than in the imaginal discs (Fig. 1g–j), similarly to the larval phenotype of *TOR* mutants[13,14]. Staining of DNA in salivary glands and fat body cells demonstrated a severe deficit in endoreplication (Fig. 1j).

The behaviour of *Rheb* mutant cells was studied during development by means of mitotic recombination. Clones of cells homozygous for EMS-induced *Rheb* alleles grew poorly and were consistently smaller than their corresponding sister clones (Fig. 2a). When provided with a proliferative advantage (by means of the Minute technique), *Rheb* mutant cells still failed to cover large regions of the

[1]Zoologisches Institut der Universität Zürich, Winterthurerstrasse 190, 8057 Zürich, Switzerland. [2]Friedrich Miescher Institute for Biomedical Research, Maulbeerstrasse 66, 4058 Basel, Switzerland. [3]The Genetics Company, Inc., Wagistrasse 27, 8952 Zürich-Schlieren, Switzerland.
Correspondence should be addressed to E. H. (hafen@zool.unizh.ch).

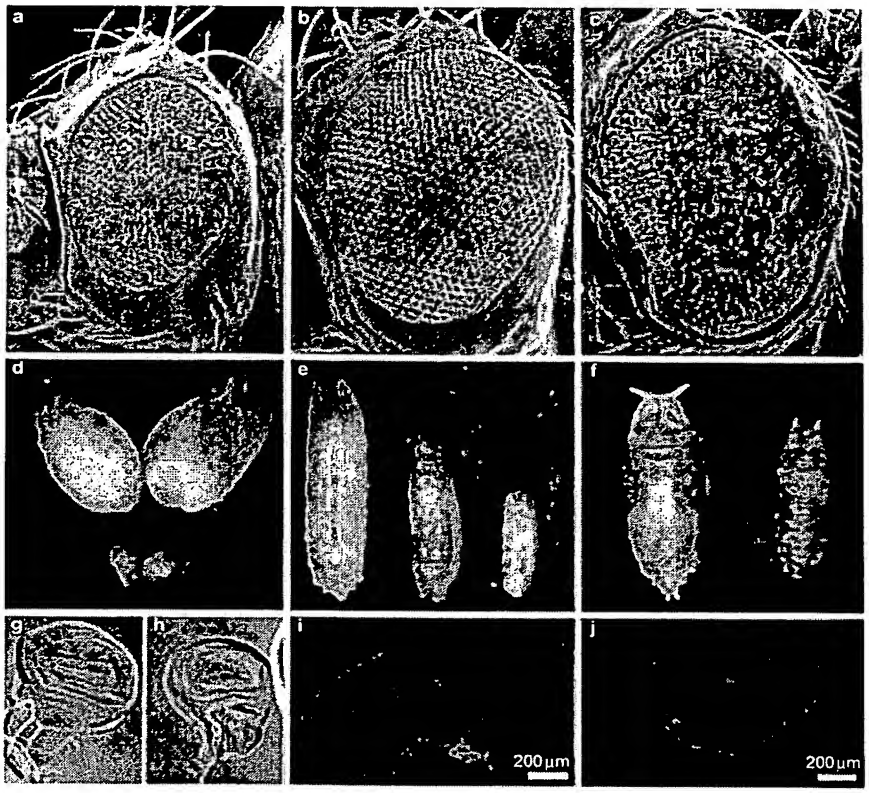

Figure 1 Growth defects caused by *Rheb* mutations. (a–c) Phenotypes that resulted in the identification of *Rheb* alleles. Shown are SEMs of female fly eyes taken at the same magnification. EMS-induced *Rheb* loss-of-function alleles were identified on the basis of the pinhead phenotype in mosaic animals with largely homozygous mutant heads, as shown in a. A comparison with a control eye, as shown in b, demonstrates the marked size reduction. An EP-element driving *Rheb* expression was isolated as a gain-of-function mutation promoting overgrowth in the eye, as shown in c. (d) Ovaries of viable $Rheb^{7A1}/Rheb^{44.1}$ females (bottom) are markedly reduced in size when compared with control ovaries (top). (e, f) Phenotype of a pupal lethal heteroallelic combination ($Rheb^{7A1}/Rheb^{26.2}$). The size range of mutant larvae (e, middle and right) is shown in comparison with a control larva (left). Whereas the smaller mutant larvae die, the larger mutant larvae arrest development at the early pupal stage. A corresponding pupa (f, right) is clearly smaller than the control pupa (left). (g–j) Size defects of imaginal discs and salivary glands in larvae of a pupal lethal heteroallelic combination ($Rheb^{3M2}/Rheb^{26.2}$). Whereas the size reduction of mutant imaginal discs is roughly proportional to the larval size (g, control; h, mutant), the salivary glands are more severely reduced (compare j to control gland in i). DAPI staining (blue) shows a strong endoreplication deficit in *Rheb* mutant salivary glands. Membranes are stained with an anti-lin7 antibody (red).

imaginal discs. Instead, the resulting clones typically displayed elongated shapes with thin extensions (Supplementary Information, Fig. S2a). A possible explanation for this unusual phenotype may reside in their attempt to minimise contact with other mutant cells. To our knowledge, this phenomenon has not been previously described in the context of growth-regulating genes. Despite this abnormal behaviour, *Rheb* mutant cells differentiate properly into adult structures. For example, analysis of clones in the adult eye revealed the presence of extremely small photoreceptor cells of otherwise normal structure and arrangement in the mutant tissue (Fig. 2b). The size reduction phenotype is strictly cell-autonomous. Taken together, the characterisation of the mutant phenotypes demonstrates that *Rheb* is required for proper growth regulation in a cell-autonomous manner.

Next, we examined whether overexpression of *Rheb* is sufficient to promote growth. The effect of overexpressing *Rheb* during development through the use of the EP 50.084 line and two independent UAS-*Rheb* lines was monitored in marked clones in imaginal discs and in the adult eye. All the lines yielded qualitatively similar results, with the EP line consistently showing the strongest effects. Clones overexpressing *Rheb* in the wing imaginal disc attained a substantially larger size when compared with control clones (Fig. 2c). This enlargement is caused by a significant increase in cell size (a 48% increase in area covered per cell). In contrast, the cell doubling time remained unchanged in cells expressing *Rheb* versus control cells (10.5 h versus 10.8 h). Consistent with the size effect in the imaginal discs, cells expressing *Rheb* in differentiating cells posterior to the morphogenetic furrow (under the control of GMR regulatory sequences) resulted in enlarged but fully differentiated photoreceptor cells (a 66% size increase of the rhabdomeres; Fig. 2d). As in the case of the loss-of-function clones, the size alteration was cell-autonomous. Thus, *Rheb* is sufficient to promote cellular growth.

As both InR and TOR signalling have been implicated in the response to nutrient availability[15,16], we asked whether overexpression of *Rheb* would promote growth even under starvation conditions. It

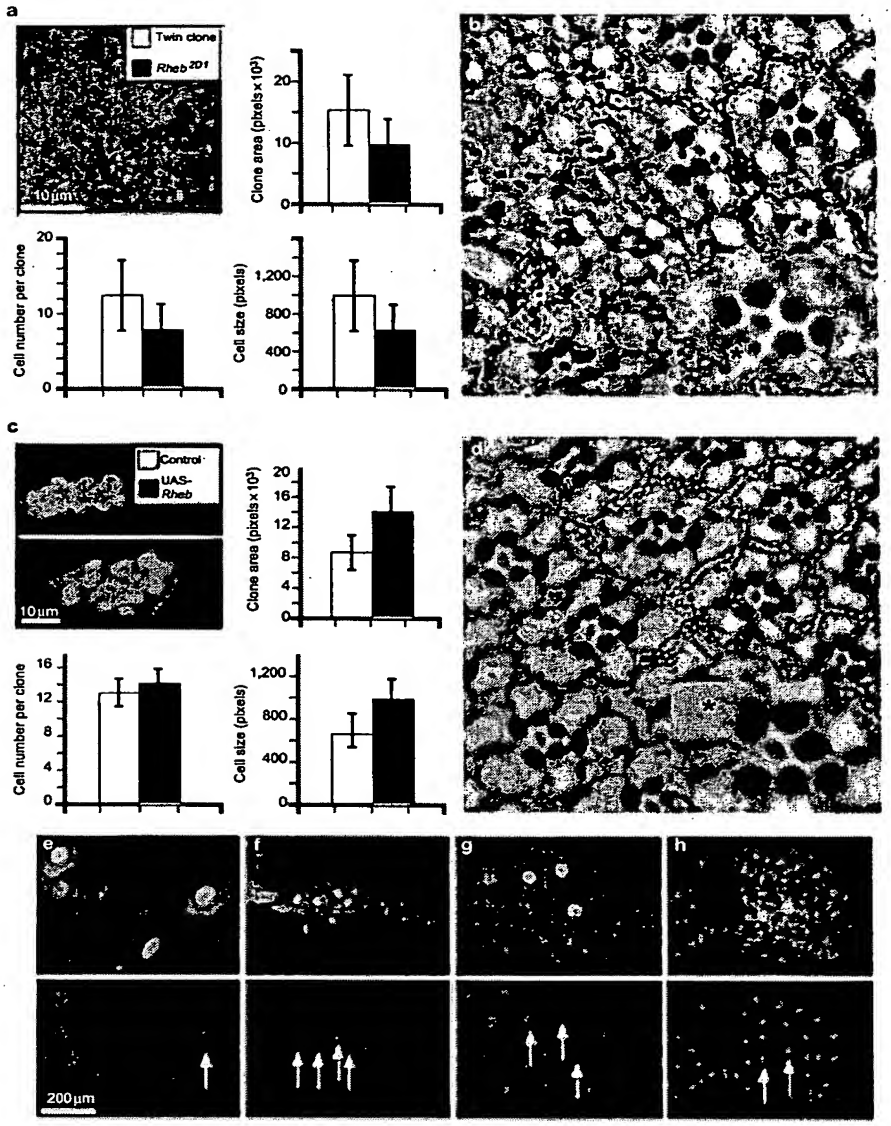

Figure 2 Clonal analysis of Rheb function. **(a)** Loss-of-function clones in the wing imaginal disc are consistently smaller than their corresponding twin clones. A clone of cells homozygous mutant for *Rheb*^{201} (marked by the absence of GFP) is only about half the size of its twin spot (bright green staining). Nuclei are labelled by DAPI staining (shown in red). The reduced clone size is accounted for by fewer and smaller cells ($n = 10$, $P = 0.00038$ for cell number, $P = 0.00126$ for cell size). **(b)** Tangential sections through compound eyes reveal that cells homozygous mutant for *Rheb*^{3M2} (marked by the lack of pigments) are able to differentiate into the various cell types of the eye. The size of the mutant cells, however, is greatly reduced (as reflected by a 72% reduction in rhabdomere area in tangential sections). A mosaic ommatidium containing a single mutant photoreceptor cell (inset, asterisk) demonstrates the cell-autonomy of the size reduction. **(c)** Flp-out clones of *Rheb*-expressing cells in the wing imaginal disc attain a significantly larger size. Clones 40 h after induction and marked by GFP expression are shown (top: control, bottom: expressing *Rheb*). The increase in clonal area is caused by larger cells ($n = 20$, $P = 0.00002$), whereas the number of cells is not significantly altered ($P = 0.087$). **(d)** Expression of *Rheb* during eye development results in an enlargement of photoreceptor cells. Cells expressing *Rheb* under GMR-control are marked by the absence of pigmentation. Cell-autonomy of the size increase is demonstrated by a single *Rheb*-expressing photoreceptor cell (asterisk) in a mosaic ommatidium (inset). **(e–h)** The effects of *Rheb* expression in endoreplicative larval tissues under normal conditions **(e, g)** and under amino-acid deprivation **(f, h)**. Cells expressing *Rheb* (labelled with GFP, arrows in lower panels) under normal nutrient availability in salivary glands **(e)** and fat body cells **(g)** display only a mild size increase. In larvae starved for amino acids, however, *Rheb* expression exerts strong effects on both cell size and DNA ploidy. In salivary glands **(f)**, *Rheb*-expressing cells display a several fold increase in size and contain much more DNA (stained with DAPI, lower panels) than non-expressing neighbouring cells, but they do not reach normal size and ploidy. In the fat body cells **(h)**, expression of *Rheb* reverts the starvation phenotype completely. Size, DNA content, and appearance (amount of vesicles) of these cells are indistinguishable from non-starved cells. Membranes are visualised with an anti-lin7 antibody staining (red). Separate DAPI staining is shown in lower panels (blue).

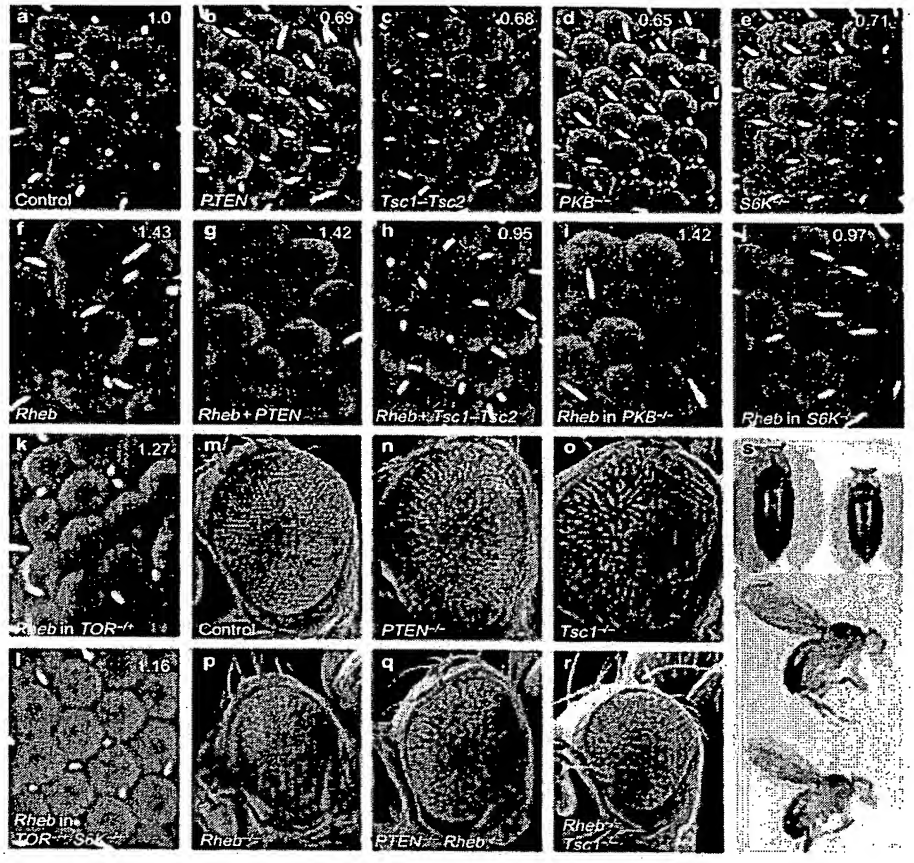

Figure 3 Epistatic relationship of Rheb with the InR/dPI(3)K and the TOR signalling pathways. (a–l) SEMs showing ommatidial size and shape of female flies. (a) Control (b) GMR-*Gal4*/+; UAS-*PTEN*/+ (c) GMR-*Gal4*/+; UAS-*Tsc1* UAS-*Tsc2*/+ (d) PKB^{1}/PKB^{3} (e) $S6K^{l\text{-}1}/S6K^{l\text{-}1}$ (f) GMR-*Gal4*/+; EP50.084/+ (g) GMR-*Gal4*/+; EP50.084/UAS-*PTEN* (h) GMR-*Gal4*/+; EP50.084/UAS-*Tsc1* UAS-*Tsc2* (i) GMR-*Gal4*/+; EP50.084 PKB^{1}/PKB^{3} (j) GMR-*Gal4*/+; $S6K^{l\text{-}1}$ EP50.084/$S6K^{l\text{-}1}$ (k) GMR-*Gal4*/TOR^{2L1}; EP50.084/+ (l) GMR-*Gal4*/TOR^{2L1}; EP50.084/$S6K^{l\text{-}1}$. Ommatidial size relative to the control is indicated in each panel. Expression of *Rheb* under GMR-*Gal4* control results in large and disorganised ommatidia (f). This phenotype can be suppressed by co-expression of *Tsc1–Tsc2* (h), but not by *PTEN* (g). The enlarged ommatidial size is still evident in a *PKB* mutant background (i), but is neutralised in flies lacking S6K function (j). The effects of *Rheb* overexpression are dominantly alleviated by TOR^{2L1} (k). (m–r) SEMs showing heads of mosaic female flies generated by the ey-Flp method. The heads are largely homozygous mutant for (m) Control (n) $PTEN^{2L117}$ (o) $Tsc1^{2G3}$ (p) $Rheb^{2D1}$ (q) $PTEN^{2L117}$ and $Rheb^{2D1}$ (r) $Rheb^{2D1}$ and $Tsc1^{2G3}$. Note that *Rheb* is epistatic over both *PTEN* and *Tsc1*, as indicated by the Rheb-like phenotype of the respective double mutants as shown in q and r. (s) Pupae doubly mutant for *Tsc1* and *Rheb* (upper panel, right) are smaller than heterozygous control pupae (left). Animals lacking Tsc1 do survive if Rheb function is compromised (lower panel, bottom). The surviving flies are slightly reduced in size when compared with the heterozygous control (top). Genotypes are: $Tsc1^{2X1}$, $Rheb^{2D1}$/*TM3* (heterozygous control animals), $Tsc1^{2X1}$, $Rheb^{2D1}/Tsc1^{1A2}$, $Rheb^{7A1}$ (doubly mutant animals).

has been shown that depriving larvae of amino acids blocks endoreplication of the larval tissues, but that this can be overcome by expression of Dp110/PI(3)K[16]. *Rheb* was expressed in small clones of cells in the salivary glands and in the fat body. Under normal food conditions, only a very subtle increase in cell size was observed (Fig. 2e, g). In larvae starved of amino acids, however, *Rheb* expression had a pronounced effect on both DNA content (as visualised by DAPI staining) and cell size (Fig. 2f, h). Despite the lack of amino acids, larval cells expressing *Rheb* reached a normal size in the fat body, and the size and endoreplication deficits were significantly alleviated in the salivary glands. We conclude that *Rheb* is sufficient to counteract the effects of amino-acid deprivation and thus may function in amino-acid sensing.

Given the similarities between *Rheb* and mutants in the InR and TOR signalling pathways, it is conceivable that Rheb represents a novel component of one of these growth control pathways. To test this possibility, a detailed epistasis analysis was performed. First, we tested whether the negative regulators of InR and TOR signalling — PTEN and Tsc1–Tsc2, respectively — could counteract the effects of *Rheb* overexpression. All overexpression experiments were performed in the eye using the GMR-*Gal4* driver line. Expression of either *PTEN* or *Tsc1–Tsc2* alone resulted in a very similar size reduction of the ommatidia (Fig. 3b, c) when compared with control ommatidia (Fig. 3a)[17–20]. However, whereas expression of *PTEN* had no influence on the increase in ommatidial size caused by *Rheb* overexpression (Fig. 3g),

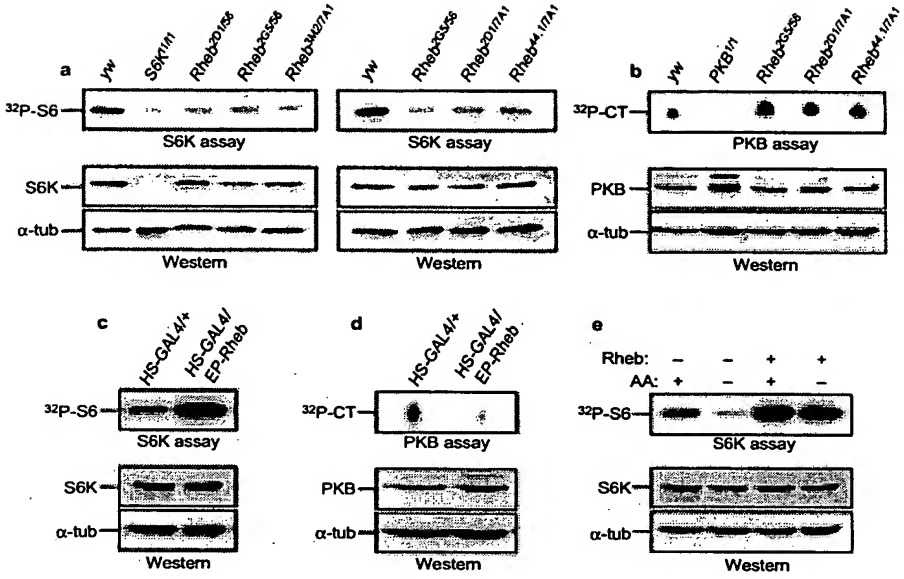

Figure 4 Rheb affects the kinase activities of S6K and PKB. (a) S6K activity depends on Rheb function. Larval extracts of various *Rheb* heteroallelic combinations were assayed for S6K kinase activity. All combinations showed a significant reduction in the kinase activity. (b) In contrast to the effect on S6K, reduction of Rheb function resulted in an increase in PKB activity. (c) Ubiquitous expression of *Rheb* resulted in a marked increase in S6K activity, accompanied by a decrease in PKB activity (d). Kinase assays were performed 7 h after heat-shock-mediated *Rheb* induction. (e) Amino-acid deprivation for 6 h (after 4 h recovery from heat-shock) did not compromise the ability of Rheb to stimulate S6K activity. Western blots of S6K and α-tubulin are shown as loading controls in the bottom panels of **a**, **c** and **e**. ^{32}P-CT: ^{32}P-Crosstide. Western blots of PKB and α-tubulin are shown as loading controls in the bottom panels of **b** and **d**.

co-expression of *Tsc1–Tsc2* resulted in ommatidia of approximately wild-type size (Fig. 3h), indicating that the activities of *Rheb* and *Tsc1–Tsc2* can counteract each other. Next, the enlarged ommatidia phenotype of GMR-*Rheb* was assayed in a number of mutant backgrounds. Reducing the activity of *Drosophila* protein kinase B (PKB) had no effect on the ommatidial size (Fig. 3i). Similar results were obtained with hypomorphic mutations in *InR* and *Dp110*, respectively (data not shown). In contrast, ommatidial size was dominantly reduced by a mutation in *TOR* (*TOR*^{2L1}; Fig. 3k), and a suppression to wild-type size was observed in a *S6K* mutant background (Fig. 3j). Thus, the *Rheb* overexpression phenotype is dependent on TOR and S6K function, but is independent of InR signal strength. Finally, we analysed the behaviour of *Rheb PTEN* and *Rheb Tsc1* double mutants. The phenotypic consequences were assayed in mosaic animals using the ey-Flp method. As expected, the *Rheb PTEN* double-mutant tissue clearly displayed a *Rheb* phenotype (Fig. 3q). The *Rheb Tsc1* mutant tissue also resembled *Rheb* single mutants (Fig. 3r), indicating that *Rheb* is epistatic over *Tsc1*.

Complete loss of Tsc1 function results in larval lethality[17,18,21]. Importantly, we found that a simultaneous reduction of *Rheb* function was sufficient to restore viability. The emerging double-mutant flies displayed a weak *Rheb* hypomorphic phenotype (a moderate size reduction; Fig. 3s). These findings suggest that the major consequence of a lack of Tsc1 is overactivation of Rheb.

Our genetic analysis indicated that Rheb regulates S6K through TOR. Therefore, we tested whether S6K activity is dependent on Rheb function. Larval extracts of various heteroallelic *Rheb* combinations were subjected to S6K and PKB kinase assays. Indeed, S6K activity was significantly reduced in all combinations without any apparent effect on S6K protein levels (Fig. 4a). PKB activity, however, was consistently increased (Fig. 4b). This is in agreement with the hypothesis that S6K is an essential component of a negative feedback loop regulating InR signalling[22,23]. Conversely, ubiquitous expression of *Rheb* resulted in an increase in S6K activity (Fig. 4c) and a concomitant decrease in PKB activity (Fig. 4d). The stimulation of S6K activity by Rheb was also observed after amino-acid deprivation (Fig. 4e). Thus, Rheb is both necessary and sufficient for S6K activation.

Although Rheb is essential for S6K activity, and the overgrowth phenotype elicited by *Rheb* overexpression depends on S6K, regulation of S6K is clearly not the only effect of Rheb activity. Whereas flies lacking S6K function are semi-viable (exhibiting a severe delay in development and a reduced body size[24]), loss of Rheb is lethal. Moreover, reduction of Rheb activity results in a decrease in cell number and cell size (as opposed to *S6K* mutants, which only affect cell size). Finally, the characteristic shape of *Rheb* mutant cell clones suggests that *Rheb* has other functions in addition to growth control.

Two models of Rheb activity can be envisaged: first, Rheb could function in the TOR signalling pathway directly downstream of and negatively regulated by Tsc1–Tsc2 (Supplementary Information, Fig. S3a). Second, Rheb might be a component of an independent pathway that impinges on S6K (Supplementary Information, Fig. S3b). In the latter model, the TOR signalling pathway and the putative parallel pathway would both be necessary for the full activation of S6K. This could explain why impairing the activity of one pathway interferes with the consequences of overactivating the other. Nevertheless, we favour the former model because *Rheb* mutants show

striking similarities with TOR signalling defects and because of the intimate genetic interactions of *Rheb* with *Tsc1–Tsc2*. A particularly attractive hypothesis implicates Tsc2 as the GAP of Rheb. Indeed, in an accompanying paper, Zhang *et al.* provide evidence that Tsc2 is the GAP for Rheb in *Drosophila* (this issue), and the same conclusion has been derived from studies on the mammalian homologues of *Drosophila* Tsc2 and Rheb (F.J.T. Zwartkruis, J.L. Bos and G.T., personal communication).

Interestingly, loss of *rhb1* function in the fission yeast *Schizosaccharomyces pombe* results in a growth arrest phenotype that is very similar to that of nitrogen-starved cells[25]. Thus, the function of Rheb in growth regulation in response to nutrients (amino acids) may have been conserved during evolution. Furthermore, the fact that impaired Rheb function is sufficient to suppress the phenotypic consequences of loss of PTEN and TSC1–TSC2 suggests that Rheb might be a suitable target for therapeutic intervention in a wide range of tumours. □

METHODS

Genetics. EMS-induced *Rheb* alleles were isolated in an *ey-Flp* mosaic screen[26] that will be described elsewhere. Two alleles, $Rheb^{2D1}$ and $Rheb^{2G5}$, were mapped genetically with respect to visible markers. A subsequent fine mapping step placed the mutations between the P-element insertions EP974 (83A3) and l(3)j1C2 (83C1-2) in a candidate region of 312.5 kb. Eight polymorphisms distributed over the candidate region were used to establish a high-resolution SNP map. The candidate region could be narrowed down to 60 kb by mapping the recombination sites between the *Rheb* alleles and the two P elements using SNP detection by DHPLC[27]. Candidate open reading frames in this interval were amplified by PCR from heterozygous *Rheb* flies and tested for polymorphisms by DHPLC. Amplified fragments of *CG1081* displayed various polymorphisms and were subsequently sequenced.

The EP line 50.084 was identified among 10,000 novel insertions of a double-headed EP element. It is inserted six nucleotides downstream of the 5′ end of the first exon of transcript CG1081-RA (GadFly database). The EP50.084 chromosome carries a closely linked lethal factor that cannot be reverted by mobilisation of the EP element. The UAS sites at the 5′ end of EP50.084 were excised by *Cre-loxP*-mediated recombination to yield a single-headed EP element capable of driving *Rheb*. EP50.084 was remobilised by crossing in the transposase source Δ2-3 to generate imprecise excision alleles. At least 83 independent reversions of the dominant $yellow^+$ marker were recovered; six of them failed to complement the *Rheb* alleles. The two imprecise excision alleles that yielded viable combinations with some EMS-alleles ($Rheb^{44.1}$ and $Rheb^{56}$) retained partial sequences of the EP element (0.6 and 1.1 kb, respectively) without deleting any flanking genomic sequences.

The following transgenes and mutations were used for interaction studies:

GMR-*Gal4* (ref. 28), UAS-*PTEN* (ref. 20), UAS-*Tsc1*, UAS-*Tsc2* (ref. 17), PKB^1 (ref. 29), PKB^3 (ref. 30), TOR^{2L1} (ref. 13), $S6K^{4-1}$ (ref. 24), $PTEN^{2L117}$ (ref. 31), $Tsc1^{2G3}$, $Tsc1^{2X1}$ and $Tsc1^{1A2}$ (H.S. and E.H., unpublished observations).

To generate loss-of-function clones, we used the lines *y w hs-Flp; FRT82 Ubi-GFP* and *y w hs-Flp; FRT82 Ubi-GFP M / TM6B* for clones in the imaginal discs, and *y w hs-Flp; FRT82* w^+ *M / TM6B* for clones in the adult eye. Clones were induced in 48–72-h-old larvae by a 45-min heat-shock at 34 °C. To circumvent potential side effects caused by second hits, at least three different EMS-induced *Rheb* alleles were tested in each experiment. The results were always qualitatively similar.

Overexpression clones were generated by means of the 'FLP-out' technique using the lines *y w hs-Flp; Act>CD2>Gal4* UAS-*GFPnls / TM6B* (ref. 32) and *y w hs-Flp;* GMR>w^+>*Gal4* (ref. 33), respectively. FLP-out clones were induced either in 80-h-old larvae by a 13-min heat-shock at 34 °C (*Act>CD2>Gal4*), or in 24–48-h-old larvae by a 1-h heat-shock at 37 °C (GMR>w^+>*Gal4*). To achieve overexpression in the endoreplicative larval tissues, spontaneous FLP-out events using *y w hs-Flp; Act>CD2>Gal4* UAS-*GFPnls / TM6B* without heat-shock application were recovered[16]. All the overexpression experiments were performed using EP50.084 and two UAS-*Rheb* lines (individually or in combination). The severity of the resulting phenotypes was always in accordance with the order EP50.084 > UAS-*Rheb13.1+14.2* > UAS-*Rheb14.2* > UAS-*Rheb13.1*, presumably reflecting different expression levels. To deprive larvae of dietary amino acids, 60-h-old larvae were incubated in 20% sucrose solution.

Eye-specific clones were generated using the ey-Flp system, as previsouly described[26]. For the double-mutant analysis of *PTEN Rheb* clones, the ey-Flp systems for 2L and 3R were combined to induce clones simultaneously for *FRT40* $PTEN^{2L117}$ and *FRT82 Rheb*. To study the effects of *Rheb Tsc1* double mutants, recombinant chromosomes were generated with various alleles.

Gal4 under control of a heat-shock promoter (*hs-Gal4*) was used to ubiquitously overexpress *Rheb*. Second-instar larvae were transferred to tubes containing fresh squashed fly food and placed in a waterbath at 37 °C for 45 min. Then larvae were allowed to recover at room temperature for the indicated times before analysis in kinase assays.

Measurements and data analysis. The body weight of male flies three days after eclosion was measured with a precision scale (Mettler Toledo, Greifensee, Switzerland). Wings of female flies were mounted and analysed as previously described[10]. Scanning electron microscope (SEM) images of five female fly eyes per genotype were analysed to characterise the eye phenotypes. Rosettes of seven ommatidia were measured using the NIH image software to determine ommatidial area.

Extraction of larvae, kinase assays and western blotting. Larvae were extracted essentially as described[13], however with a modified extraction buffer (120 mM sodium chloride, 50 mM Tris-HCl at pH 7.0, 20 mM sodium fluoride, 1 mM benzamidine, 1 mM EDTA, 6 mM EGTA, 15 mM $Na_4P_2O_7$-$10H_2O$ and 1% NP-40; the following reagents were added shortly before use to the indicated concentrations: 1/5 volume Complete Mini protease inhibitor cocktail (Roche Diagnostics, Rotkreuz, Switzerland) prepared as a 5× stock in extraction buffer without the reagents listed hereafter, 2 mM AEBSF (Pefabloc SC (Roche)), 30 mM *para*-nitrophenylphosphate, 30 mM β-glycerolphosphate, 4 μM leupeptin, 2 μM aprotinin, 4 μM pepstatin and 100 μM phenyl methylsulphonyl fluoride).

Kinase activity assays of either S6K or PKB were performed as described[13,22].

For immunoblotting, the following antibodies were used at the indicated dilutions: S6K D-20 antibody at 1:200 (ref. 24), PKB antibody (ref. 34) at 1:1000 and α-tubulin antibody (Sigma, St Louis, MO) at 1:1000. HRP-conjugated secondary antibodies (Dako A/S, Glostrup, Denmark) were diluted 1:2000. Signals were detected using ECL western blotting detection reagents (Amersham Biosciences, Little Chalfont, Buckinghamshire, UK).

Note: Supplementary Information is available on the Nature Cell Biology website.

ACKNOWLEDGEMENTS

We thank R. Bopp, D. El Tounsy Garner, P. Wüstemann, P. Gast, E. Niederer and C. Hugentobler for technical assistance; N. Tapon, I. Hariharan, B. Edgar, T. Xu, B. Dickson and the Bloomington Stock Center for flies; B. Hemmings and A. Hajnal for antibodies; K. Basler for critically reading the manuscript, and B. Edgar, D. Pan and N. Tapon for communicating results prior to publication. This work was supported by grants from the Swiss National Science Foundation (to E.H.), the Swiss Cancer League (to G.T. and E.H.) and the Roche Research Foundation (to T.R.).

COMPETING FINANCIAL INTERESTS

The authors declare that they have no competing financial interests.

Received 10 February 2003; Accepted 24 April 2003;
Published online: 27 April 2003; DOI: 10.1038/ncb995

1. Potter, C. J. & Xu, T. Mechanisms of size control. *Curr. Opin. Genet. Dev.* **11**, 279–286 (2001).
2. Johnston, L. A. & Gallant, P. Control of growth and organ size in *Drosophila*. *Bioessays* **24**, 54–64 (2002).
3. Marygold, S. & Leevers, S. Growth signaling: TSC takes its place. *Curr. Biol.* 12, R785–R787 (2002).
4. McManus, E. J. & Alessi, D. R. TSC1–TSC2: a complex tale of PKB-mediated S6K regulation. *Nature Cell Biol.* 4, E214–E216 (2002).
5. Radimerski, T., Montagne, J., Hemmings-Mieszczak, M. & Thomas, G. Lethality of *Drosophila* lacking TSC tumor suppressor function rescued by reducing dS6K signaling. *Genes Dev.* **16**, 2627–2632 (2002).
6. Oldham, S. & Hafen, E. Insulin/IGF and target of rapamycin signaling: a TOR de force in growth control. *Trends Cell Biol.* **13**, 79–85 (2003).
7. Leslie, N. R. & Downes, C. P. PTEN: The down side of PI 3-kinase signalling. *Cell.*

Signal. **14**, 285–295 (2002).
8. Wienecke, R., Konig, A. & DeClue, J. E. Identification of tuberin, the tuberous sclerosis-2 product. Tuberin possesses specific Rap1GAP activity. *J. Biol. Chem.* **270**, 16409–16414 (1995).
9. Xiao, G. H., Shoarinejad, F., Jin, F., Golemis, E. A. & Yeung, R. S. The tuberous sclerosis 2 gene product, tuberin, functions as a Rab5 GTPase activating protein (GAP) in modulating endocytosis. *J. Biol. Chem.* **272**, 6097–6100 (1997).
10. Böhni, R. *et al.* Autonomous control of cell and organ size by CHICO, a *Drosophila* homolog of vertebrate IRS1-4. *Cell* **97**, 865–875 (1999).
11. Brogiolo, W. *et al.* An evolutionarily conserved function of the *Drosophila* insulin receptor and insulin-like peptides in growth control. *Curr. Biol.* **11**, 213–221 (2001).
12. Yamagata, K. *et al. rheb*, a growth factor- and synaptic activity-regulated gene, encodes a novel Ras-related protein. *J. Biol. Chem.* **269**, 16333–16339 (1994).
13. Oldham, S., Montagne, J., Radimerski, T., Thomas, G. & Hafen, E. Genetic and biochemical characterization of dTOR, the *Drosophila* homolog of the target of rapamycin. *Genes Dev.* **14**, 2689–2694 (2000).
14. Zhang, H., Stallock, J. P., Ng, J. C., Reinhard, C. & Neufeld, T. P. Regulation of cellular growth by the *Drosophila* target of rapamycin dTOR. *Genes Dev.* **14**, 2712–2724 (2000).
15. Gao, X. *et al.* Tsc tumour suppressor proteins antagonize amino-acid-Tor signaling. *Nature Cell Biol.* **4**, 699–704 (2002).
16. Britton, J. S., Lockwood, W. K., Li, L., Cohen, S. M. & Edgar, B. A. *Drosophila*'s insulin/PI3-kinase pathway coordinates cellular metabolism with nutritional conditions. *Dev. Cell* **2**, 239–249 (2002).
17. Tapon, N., Ito, N., Dickson, B. J., Treisman, J. E. & Hariharan, I. K. The *Drosophila* tuberous sclerosis complex gene homologs restrict cell growth and cell proliferation. *Cell* **105**, 345–355 (2001).
18. Potter, C. J., Huang, H. & Xu, T. *Drosophila* Tsc1 functions with Tsc2 to antagonize insulin signaling in regulating cell growth, cell proliferation, and organ size. *Cell* **105**, 357–368 (2001).
19. Gao, X., Neufeld, T. P. & Pan, D. *Drosophila* PTEN regulates cell growth and proliferation through PI3K-dependent and -independent pathways. *Dev. Biol.* **221**, 404–418 (2000).
20. Huang, H. *et al.* PTEN affects cell size, cell proliferation and apoptosis during *Drosophila* eye development. *Development* **126**, 5365–5372 (1999).
21. Gao, X. & Pan, D. TSC1 and TSC2 tumor suppressors antagonize insulin signaling in cell growth. *Genes Dev.* **15**, 1383–1392 (2001).
22. Radimerski, T. *et al.* dS6K regulated cell growth is dPKB/dPI3K independent, but requires dPDK1. *Nature Cell Biol.* **4**, 251–255 (2002).
23. Haruta, T. *et al.* A rapamycin-sensitive pathway down-regulates insulin signaling via phosphorylation and proteasomal degradation of insulin receptor substrate-1. *Mol. Endocrinol.* **14**, 783–794 (2000).
24. Montagne, J. *et al. Drosophila* S6 Kinase: A Regulator of Cell Size. *Science* **285**, 2126–2129 (1999).
25. Mach, K. E., Furge, K. A. & Albright, C. F. Loss of Rhb1, a Rheb-related GTPase in fission yeast, causes growth arrest with a terminal phenotype similar to that caused by nitrogen starvation. *Genetics* **155**, 611–622 (2000).
26. Newsome, T. P., Asling, B. & Dickson, B. J. Analysis of *Drosophila* photoreceptor axon guidance in eye-specific mosaics. *Development* **127**, 851–860 (2000).
27. Nairz, K., Stocker, H., Schindelholz, B. & Hafen, E. High-resolution SNP mapping by denaturing HPLC. *Proc. Natl Acad. Sci. USA* **99**, 10575–10580 (2002).
28. Hay, B. A., Wassarman, D. A. & Rubin, G. M. *Drosophila* homologs of baculovirus inhibitor of apoptosis proteins function to block cell death. *Cell* **83**, 1253–1262 (1995).
29. Staveley, B. E. *et al.* Genetic analysis of protein kinase B (AKT) in *Drosophila*. *Curr. Biol.* **8**, 599–602 (1998).
30. Stocker, H. *et al.* Living with lethal concentrations of PIP3: A mutation in the PH domain of Akt/PKB restores the viability of flies lacking the tumor suppressor PTEN. *Science* **295**, 2088–2091 (2002).
31. Oldham, S. *et al.* The *Drosophila* insulin/IGF receptor controls growth and size by modulating PtdInsP3 levels. *Development* **129**, 4103–4109 (2002).
32. Neufeld, T. P., Delacruz, A. F. A., Johnston, L. A. & Edgar, B. A. Coordination of Growth and Cell Division in the *Drosophila* Wing. *Cell* **93**, 1183–1193 (1998).
33. Rintelen, F., Stocker, H., Thomas, G. & Hafen, E. PDK1 regulates growth through PKB and S6K in *Drosophila*. *Proc. Natl Acad. Sci. USA* **98**, 15020–15025 (2001).
34. Andjelkovic, M. *et al.* Developmental regulation of expression and activity of multiple forms of the *Drosophila* RAC protein kinase. *J. Biol. Chem.* **270**, 4066–4075 (1995).
35. Potter, C. J., Pedraza, L. & Xu, T. Akt regulates growth by directly phosphorylating Tsc2. *Nature Cell Biol.* **4**, 658–665 (2002).